Journal of Advances in Mathematics and Computer Science

35(3): 26-45, 2020; Article no.JAMCS.56986

ISSN: 2456-9968

(Past name: British Journal of Mathematics & Computer Science, Past ISSN: 2231-0851)

A Formal Homogenization Approach to Piping Flow Erosion with Deposition in a Spatially Heterogeneous Soil

Adu Sakyi[1*], Peter Amoako-Yirenkyi[1] and Isaac Kwame Dontwi[1]

[1] *Department of Mathematics, Kwame Nkrumah University of Science and Technology, Center for Scientific and Technical Computing, National Institute for Mathematical Sciences, Kumasi, Ghana.*

Authors' contributions

This work was carried out in collaboration among all authors. AS(PhD) designed the study, performed the numerical analysis, wrote the protocol, and wrote the first draft of the manuscript. PAY(PhD) and IKD(Prof.) managed the technicalities in the analyses of the study and further guided the research. All authors read and approved the final manuscript.

Article Information

DOI: 10.9734/JAMCS/2020/v35i330257

Editor(s):

(1) Dr. Rodica Luca, Technical University Gheorghe Asachi Iasi, Romania.

Reviewers:

(1) E. H. Etuk, Rivers State University, Nigeria.

(2) Mostafa El Moumni, University Chouaib Doukkali, Morocco.

Complete Peer review History: http://www.sdiarticle4.com/review-history/56986

Original Research Article

Received: 09 March 2020

Accepted: 14 May 2020

Published: 29 May 2020

Abstract

We model and simulate piping erosion phenomena with deposition in a spatially heterogeneous soil mass motivated by seepage flow. The soil is considered to be a porous media with periodic positioning of pores spread around cylindrical structures or microstructures making the heterogeneities periodic in space.The period of the heterogeneities defines a microscopic length scale ϵ of the microscopic problem and this allows the use of periodic homogenization methods. We studied the asymptotic behaviour of the solutions to the micro problem as $\epsilon \to 0$ and obtained a homogenized model or macro problem with explicit formula for effective coefficients. Numerical simulations of the proposed model captures the expected behaviour of soil particle concentration and deposition as observed in piping flow erosion phenomena.

Keywords: Homogenization; piping flow erosion; deposition; entrainment; microscopic scale; macroscopic scale.

**Corresponding author: E-mail:asakyi10@gmail.com, asakyi@nims.edu.gh;*

1 Introduction

In many parts of the world where heavy rainfall is frequently experienced, erosion on yearly basis destroys infrastructure in both urban areas and villages normally threatening important cultural and historical resources as well. For example a community in Ghana which had a 5km shoreline was reduced to 40m by 2016 due to erosion [1, 2]. Severe erosion accompanied by gulley formation is widespread and therefore a pressing subject in many parts of the world where there are consistent heavy rainfall. While erosion is mainly a natural process, activities of humans have heightened their impact [3].The Food and Agriculture Organization led Global Soil Partnership reports that 75 billion tonnes of soil are eroded every year from arable lands worldwide. Severe erosion accompanied by gulley formation is widespread throughout Ghana [4, 5].

Both internal soil erosion and even soil surface run-offs are major cause of failures in hydraulic structures such as dikes or dams. One of the major cause of flooding is the absence or breakdown of existing Flood defence systems normally constructed using dams, dikes, storm rise barriers and dunes. These defence systems do not always hold or fail resulting in catastrophic outcomes. Typical example includes the 2005 flooding in United States of America[6], Pakistan in 2010, Thailand and Japan in 2011, Accra-Ghana in 2015 [7]. These hydraulic facility failures are mainly due to piping thus soil particles are washed from the subsoil by a ground water flow instigated by seepages [8, 9]. Although piping is a known cause of hydraulic failures, a lot of attention for their design has been given to height and slope stability with a wealth of research on surface erosion [10, 11, 12]. Our minds mostly reflects on surface erosion any time erosion comes into play, internal erosion however is most deadly as one might not know the process has initiated until breach sets in [13]. Piping erosion is an internal mechanism. According to [14], for piping flow erosion to occur, four conditions must exist. First, a sufficient hydraulic head is required as the driving force for the process. Secondly, there must be an erodible material within flow path which must be carried by the seepage flow. for the eroded materials to escape there must be an unprotected exit and lastly, the material being piped must be able to form a roof for the pipe.[15] reported that forty-Six (46) percent of dam failures are caused by piping. Also [16] studied Seventy-Four (74) Basins in Britain and found that Thirty (30) percent were receptive to piping.

In spite of the availability of a number of models [17] for dealing with aspects of erosion only few mathematical models are available to ideally describe the main mechanisms associated with internal erosion process due to the complexity of piping [18]. In 2010, experimental results obtained in [19] established the effect of spatial variability on erosion rate estimation and implied the influence of spatial heterogeneities of soil properties. Deposition effect on the flow phenomena has also been reported by [20] where the soil-fluid interface velocity was expressed as a function of mass flux which affects the erosion process. However the existing mathematical models [21, 18, 22] developed for internal erosion under axial and radial flow conditions, the erosion process is assumed to involve a smooth transformation from solid-like to fluid-like conduct. In [8] and subsequently in [23] the respective authors used two-phase flow equations with a sharp fluid-soil interface to model flow and erosion in soil pipe. The model developed remains the closest model for internal erosion under axial and radial flow conditions where erosion process was not assumed to involve a smooth transformation from solid-like to fluid-like conduct. Nonetheless, Sedimentation and deposition processes were still neglected. The soil structure was also assumed saturated and homogeneous so influences of spatial heterogeneities of soil properties were also ignored.

Modeling of the piping phenomenon is essential in order to understand the mechanisms involved. The problem is complex because erosion involves the interaction of a fluid usually water with the ground (soil). The soil and action of water on the ground can be seen in various ways. It is clear that, the basic models have been done but a more general approach is essential to deeply understand the piping mechanism. With mathematical homogenization as a tool and using specific

properties of periodic functions in combination with regularity of the weak solutions to the PDE models obtained, we propose in this paper a model for simulating the piping flow phenomena in a spatially heterogeneous soil. We consider the spatial variability of the properties of the porous medium and in addition incorporate the pore space dynamics due to deposition of fines in the flow paths.

1.1 An overview of the homogenization process

Homogenization is an approach that studies the macro behaviour of a medium by its micro properties thus the method seeks to replace a heterogeneous material by an equivalent homogeneous one. The heterogeneous medium is described as a medium with local parameters that can be described by functions rapidly varying with respect to space variables and time. Hence it can be modelled with partial differential equations which have oscillating coefficients. Under periodicity assumptions the system of partial differential equations (PDE) representing the physical phenomena usually takes the form

$$A^{\epsilon}u^{\epsilon} = B \ in \ \Omega \tag{1.1}$$

where A^{ϵ} is a partial differential operator with periodic coefficients, B is a source term, u^{ϵ} is a solution to the system, Ω the spatial domain and ϵ a scaled parameter. We aim to replace (1.1) with a continuum model in an equivalent macroscopic medium

$$\bar{A}u = B \ in \ \Omega \tag{1.2}$$

with $\bar{A}$ being a homogenized operator and u a homogenized limit of u^{ϵ} which can be achieved using an asymptotic expansion in terms of ϵ and averaging with respect to y [24, 25]. This approach by asymptotic expansion can be justified mathematically by rigorous use of periodic homogenization [26, 27]. An important proven statement on homogenization is given in *Theorems* 1.1 and 1.2.

Theorem 1.1. *Let $u^{\epsilon}(t,x,y)$ be a bounded sequence in $L^2(F;L^2(\Omega))$ (Ω an open set in $\mathbf{R^N}$, $F = (0,t)$ for $t \in (0,\infty)$). There exist a subsequence, still denoted by u^{ϵ}, and a function $u_0(t,x,y) \in L^2(F;L^2(\Omega \times Y))$ ($Y = (0,1)^N$ a unit cube) such that*

$$\lim_{\epsilon \to 0} \int_F \int_\Omega u^{\epsilon}\rho(t,x,\tfrac{x}{\epsilon})dxdt = \tfrac{1}{|Y|} \int_F \int_\Omega \int_Y u_0(t,x,y)\rho(t,x,y)dydxdt$$

for all $\rho \in C_0^{\infty}(F \times \Omega, C^{\infty}(Y))$. Such a sequence u^{ϵ} is said to two-scale converge to $u_0(t,x,y)$.

Theorem 1.2. *Let u^{ϵ} be a sequence that two-scale converges to $u_0(t,x,y)$. Then, u^{ϵ} weakly converges in $L^2(F \times \Omega)$ to $u(t,x) = \int_Y u_0(t,x,y)dy$, and we have*

$$\lim_{\epsilon \to 0} ||u^{\epsilon}||_{L^2(F\times\Omega)} \geq ||u_0||_{L^2(F\times\Omega\times Y)} \geq ||u||_{L^2(F\times\Omega)}$$

Furthermore if equality is achieved

$$\lim_{\epsilon \to 0} ||u^{\epsilon}||_{L^2(F\times\Omega)} = ||u_0||_{L^2(F\times\Omega\times Y)}$$

and if $u_0(t,x,y)$ is smooth, then we have

$$\lim_{\epsilon \to 0} ||u^{\epsilon} - u_0||_{L^2(F\times\Omega\times Y)} = 0$$

2 Formulation of the Microscopic problem

We consider a bounded soil structure Λ in $\mathcal{R}^2$ of coordinates $x = (x_1, x_2)$ through which a water/soil particles mixture of volume Λ_f flows through a soil matrix Λ_s, we define a fluid/soil interface $\partial\Lambda_s$ (purely geometrical with no thickness). We call the spatial variable x , a macroscale (global) variable. The size of the soil domain is considered to be a heterogeneous porous medium with periodic positioning of pores spread around cylindrical structures.The flow considered is two phase

(water and soil), thus the water erode the soil and entrain the eroded soil thereby creating a tunnel beneath the hydraulic structure. Pore spaces are classified into clogged and non-clogged conduit hence in the process surface deposits and clog deposits occur resulting in a change in pore structure. As soil particles build up in the clogged conduit flow is diverted to the remaining bare fluid pathway.

2.1 Choice of the micro structure: Basic geometry

We take in the space $\mathcal{R}^2$ a unit cell Y with a microscale (local) variable $y = (y_1, y_2)$, define a characteristic length scale $\epsilon = \dfrac{l}{L}$ with $y_i = \frac{x_i}{\epsilon}$ for $i \in \{1, 2\}$ where l and L denote the characteristic length of the unit cell Y and the soil domain Λ. The reference unit cell Y has two pairwise disjoint connected domains Y^s and Y^f with smooth fluid/soil boundary ∂Y^s. Next we create a repeating arrangement of copies ϵY occupying the entire region Λ as shown in Fig. 1.

For $Y \subset \mathcal{R}^2$ we define a shifted subset

$Y_k = Y + \sum_{i=1}^{2} k_i e_i$ for $k = (k_1, k_2) \in \mathcal{R}^2$, $e = (e_1, e_2)$ unit vectors in $\mathcal{R}^2$. The pore matrix (skeleton)

$$\Lambda_s^\epsilon = \bigcup_{k \in \mathcal{R}^2} \{\epsilon Y_k^s : Y_k^s \subset \Lambda\}$$

The fluid part of the domain $\Lambda_f^\epsilon = \Lambda \backslash \Lambda_s^\epsilon$ with $\Lambda_f^\epsilon \cup \Lambda_s^\epsilon = \Lambda^\epsilon \subset \Lambda$. The total geometrical surface of the skeleton

$$\partial\Lambda_s^\epsilon = \bigcup_{k \in \mathcal{R}^2} \{\epsilon \partial Y_k^s : \partial Y_k^s \subset \Lambda\}$$

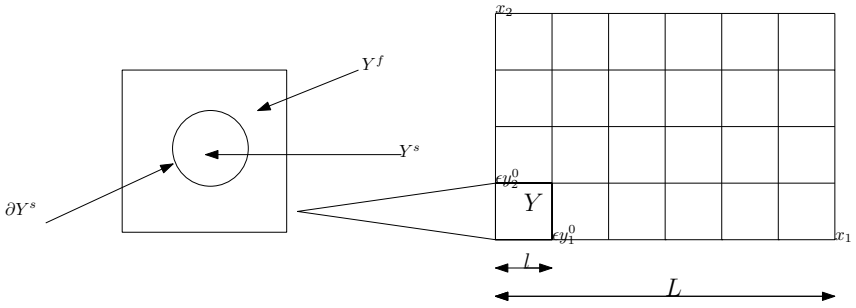

Fig. 1. (a) Left: Reference unit cell Y. (b) Right: Micro-scale geometry of the soil domain Λ^ϵ

2.2 Proposed Microscopic model

We define in the parameterized domain Λ^ϵ flow velocity $\mathbf{u^\epsilon(t,x,y)}$, concentration of soil particles in fluid-solid mixture $\mathbf{C_s^\epsilon(t,x,y)}$, concentration of deposited soil particles $\mathbf{S_d^\epsilon(t,x,y)}$, flow pressure $\mathbf{p^\epsilon(t,x,y)}$, diffusion coefficient $\mathbf{D(t,y)}$, molecular viscosity $\boldsymbol{\mu}\mathbf{(t,y)}$, a unit normal to the geometrical interface $\mathbf{n}$, Euler number $E_u(t, y)$, velocity at the geometrical interface $u^{\partial\Lambda_s}$, attachment efficiency for non-clogging and clogging conduit respectively β_{nc} and β_{cl}, average overall mass transfer coefficient Ψ, fraction of non-clogging conduit $f_{nc}^\epsilon(t.x, y)$. Combining fundamental theories of mass transfer in porous media, hydrodynamics and assuming there is no colloidal interaction energy and that diffusion and advection are of same order of magnitude we obtain the following governing equations with boundary conditions for $t \in (0, \infty)$ in an Eulerian framework after the nondimensionalization with the dimensionless quantities specified in Table 1.

Table 1. Table of dimensionless quantities: $t_{er}, u_c, D_0, C_0, p_c, l_c$ being reference (characteristic) quantities

Variables	SI units	Dimensionless form
time	s	$t = \dfrac{\mathbf{t}}{t_{er}}$
velocity	ms^{-1}	$u = \dfrac{\mathbf{u}}{u_c}$
Molecular Viscosity	$kgs^{-1}m^{-1}$	$\mu = \dfrac{\boldsymbol{\mu}}{\rho_f u_c l_c}$
Solid Concentration	kgm^{-3}	$C_s = \dfrac{\mathbf{C_s}}{C_0}$
Solid Deposited	kgm^{-3}	$S_d = \dfrac{\mathbf{S_d}}{C_0}$
Pressure	$kgm^{-1}s^{-2}$	$p = \dfrac{\mathbf{p}}{p_c}$
Diffusion Coefficient	m^2/s	$D = \dfrac{\mathbf{D}}{D_0}$

Mass Balance equation for the mixture:

$$\nabla . u^{\epsilon} = 0 \ \ in \ \ \Lambda^{\epsilon} \tag{2.1}$$

$$[\rho(u^{\epsilon\partial\Lambda_s} - u^{\epsilon}).n] = 0 \quad on \ \ \partial\Lambda_s^{\epsilon} \tag{2.2}$$

Conservation of Mass of soil particles concentration with deposition (mixture):

$$\frac{\partial}{\partial t}(C_s^{\epsilon} + S_d^{\epsilon}) + \nabla.(u^{\epsilon}C_s^{\epsilon}) = \nabla.(D(t,y)\nabla C_s^{\epsilon}) \quad in \ \ \Lambda_f^{\epsilon} \tag{2.3}$$

$$[C_s^{\epsilon}(u^{\epsilon\partial\Lambda_s} - u^{\epsilon}) + D(t,y)\nabla C_s^{\epsilon}].n = 0 \quad on \ \ \partial\Lambda_s^{\epsilon} \tag{2.4}$$

Equation of motion of Mixture:

$$\frac{\partial}{\partial t}(u^{\epsilon}) + (u^{\epsilon}.\nabla)u^{\epsilon} = -E_u(t,y)\nabla p^{\epsilon} + \nabla.(2\mu(t,y)\nabla u^{\epsilon}) \quad in \ \ \Lambda_f^{\epsilon} \tag{2.5}$$

$$[u^{\epsilon}(u^{\epsilon\partial\Lambda_s} - u^{\epsilon}) - E_u(t,y)p^{\epsilon} + 2\mu(t,y)\nabla u^{\epsilon}].n = 0 \quad on \ \ \partial\Lambda_s^{\epsilon} \tag{2.6}$$

Rate of deposition of soil particles:

$$\frac{\partial S_d^{\epsilon}}{\partial t} = (\beta_{nc} f_{nc}^{\epsilon} + \beta_{cl}(1 - f_{nc}^{\epsilon}))\Psi C_s^{\epsilon} \ \ in \ \ \Lambda_f^{\epsilon} \tag{2.7}$$

Rate of decrease in the fraction of non-clogging conduit:

$$\frac{\partial f_{nc}^{\epsilon}}{\partial t} + \beta_{nc}\Psi f_{nc}^{\epsilon} C_s^{\epsilon} = 0 \ \ in \ \ \Lambda_s^{\epsilon} \tag{2.8}$$

3 Formal Homogenization of the Microscopic Problem

The aim is to obtain a macroscopic model using asymptotic analysis of the characteristic length scale ϵ of the micro structure. We seek to replace the rapidly varying coefficients of the microstructure with an effective homogenized coefficients by averaging out the periodicity through homogenization. Define a Hilbert Space $Q(Y) = \{m \in H^1(Y) : m \ is \ Y - periodic; \frac{1}{|Y|}\int_Y m dy = 0 \ \}$ for Y-periodic functions and assume D, $\mu \in L^{\infty}(\Lambda^{\epsilon})$ and are symmetric positive definite. Also for a Y-periodic

For any quantity a, a^{ϵ} is the parameterized form of a, also $[a] = a_{flow} - a_{soil}$

vector field $(f_i(y))$ we have $\int_Y \frac{\partial f_i}{\partial y_i} dy = \int_{\partial Y} f_i n_i ds = 0$. We employ the homogenization ansatz thus our solution at the microscopic level can be expressed as a series of smooth functions and the characteristic length scale ϵ.

$$u^{\epsilon}(t,x) = u_0(t,x,y) + \epsilon u_1(t,x,y) + \epsilon^2 u_2(t,x,y) + O(\epsilon^3) \tag{3.1}$$

$$C_s^{\epsilon}(t,x) = C_{s0}(t,x,y) + \epsilon C_{s1}(t,x,y) + \epsilon^2 C_{s2}(t,x,y) + O(\epsilon^3) \tag{3.2}$$

$$S_d^{\epsilon}(t,x) = S_{d0}(t,x,y) + \epsilon S_{d1}(t,x,y) + \epsilon^2 S_{d2}(t,x,y) + O(\epsilon^3) \tag{3.3}$$

$$p^{\epsilon}(t,x) = p_0(t,x,y) + \epsilon p_1(t,x,y) + \epsilon^2 p_2(t,x,y) + O(\epsilon^3) \tag{3.4}$$

$$f_{nc}^{\epsilon}(t,x) = f_{nc_0}(t,x,y) + \epsilon f_{nc_1}(t,x,y) + \epsilon^2 f_{nc_2}(t,x,y) + O(\epsilon^3) \tag{3.5}$$

where $u_i(t,x,y), C_{si}(t,x,y), S_{di}(t,x,y)$, $f_{nc_i}(t,x,y)$ and $p_i(t,x,y)$ are $Y-periodic$. The homogenization method as in [27] consists of substituting these expansions into the dimensionless systems ((2.1) - (2.8)) and identifying the powers of ϵ. Due to the choice of the microscopic scale and the two spatial variables, the spatial derivatives take the form :

$$\nabla = \nabla_x + \frac{1}{\epsilon}\nabla_y \tag{3.6}$$

3.1 Homogenization of the mass balance equation

Using (3.1) on (2.1) and (2.2) and identifying the powers of ϵ we obtain in Y^f:

$$\begin{aligned} \nabla_y.u_0 &= 0 && (3.7)\\ \nabla_x.u_0 + \nabla_y.u_1 &= 0 && (3.8)\\ \nabla_x.u_1 + \nabla_y.u_2 &= 0 && (3.9)\\ \nabla_x.u_2 &= 0 && (3.10) \end{aligned}$$

with boundary condition at ∂Y^s:

$$\begin{aligned} (u_0^{\partial Y_s} - u_0).n(y) = 0 && (3.11)\\ (u_1^{\partial Y_s} - u_1).n(y) = 0 && (3.12)\\ (u_2^{\partial Y_s} - u_2).n(y) = 0 && (3.13) \end{aligned}$$

3.2 Homogenization of the soil particle concentration with deposition equation

Applying the homogenization ansatz in (3.1), (3.2),(3.3) on (2.3),(2.4) and collecting powers of ϵ after using (3.11),(3.12) and (3.13) we obtain the boundary value problems.

By definition ∇_x,∇_y denote the gradients with respect to x and y respectively, and $\frac{\partial}{\partial t}$ denoted as ∇_t

3.2.1 Boundary value problem for C_{s0}:

$$P^c_{-2}\begin{cases} Find\ C_{s0}=C_{s0}(t,x,y)\ such\ that \\ \nabla_y.D(t,y)\nabla_y C_{s0}=0\ in\ Y^f \\ D(t,y)\nabla_y C_{s0}=0\ on\ \partial Y^s \\ C_{s0}=C_{s0}(t,x,y)\ is\ Y-periodic \end{cases} \tag{3.14}$$

The structure of P^c_{-2} portrays C_{s0} and is independent of y hence the solution must be of the form

$$C_{s0}(t,x,y)=C_{s0}(t,x) \tag{3.15}$$

the existence and uniqueness of (3.15) is guaranteed via Lax-Milgram theorem.

3.2.2 Boundary value problem for C_{s1}

The second order C_{s1} satisfies:

$$P^c_{-1}\begin{cases} Find\ C_{s1}=C_{s1}(t,x,y)\ such\ that \\ -\nabla_y.(D(t,y)(\nabla_x C_{s0}+\nabla_y C_{s1}))=0\ in\ Y^f \\ D(t,y)(\nabla_x C_{s0}+\nabla_y C_{s1}).n(y)=0\ on\ \partial Y^s \\ C_{s1}=C_{s1}(t,x,y)\ is\ Y-periodic \end{cases} \tag{3.16}$$

P^c_{-1} is linear, by the method of separation of variables we can write the solution to the linear problem in the form:

$$C_{s1}(t,x,y)=\bar{C}_{s1}(t,x)+\sum_{j=1}^{2}\nabla_{x_j}C_{s0}(t,x)\chi^c_j(y) \tag{3.17}$$

Where $\chi^c_j(y)=\begin{bmatrix}\chi^c_1(y)\\ \chi^c_2(y)\end{bmatrix}\in\mathbb{R}^2$ are cell functions, $\bar{C}_{s1}$ is an arbitrary function of x and t. From (3.17) we note that $\nabla_y C_{s1}(t,x,y)=\sum_{j=1}^{2}\nabla_{x_j}C_{s0}(t,x)\nabla_y\chi^c_j(y)$ and $\nabla_x C_{s0}(t,x)=\sum_{j=1}^{2}\nabla_{x_j}C_{s0}(t,x)\bar{e}_j$,hence from (3.16) we obtain what we call the cell problem from which we can compute $\chi^c_j(y)$:

$$P^c_{-1,j}\begin{cases} -\nabla_y.(D(t,y)(\bar{e}_j+\nabla_y\chi^c_j(y))=0\ in\ Y^f \\ D(t,y)(\bar{e}_j+\nabla_y\chi^c_j(y)).n(y)=0\ on\ \partial Y^s \\ \chi^c_j\ is\ Y-periodic \end{cases} \tag{3.18}$$

3.2.3 Boundary value problem (BVP) for C_{s2}

Finally the BVP for the third order C_{s2}:

$$P^c_0\begin{cases} \nabla_t(C_{s0}+S_{d0})-\nabla_x.(D(t,y)(\nabla_x C_{s0}+\nabla_y C_{s1}))- \\ \nabla_y.(D(t,y)(\nabla_x C_{s1}+\nabla_y C_{s2}))+\nabla_x.(u_0C_{s0})+\nabla_y.(u_0C_{s1})=0\ in\ Y^f \\ D(t,y)(\nabla_x C_{s1}+\nabla_y C_{s2}).n(y)=0\ on\ \partial Y^s \\ C_{s2}(t,x,y)\ is\ Y-periodic \end{cases} \tag{3.19}$$

We integrate (3.19) over the $Y-cell$ and averaging with respect to y

P^c_a for $a\in\mathbf{R}$ denote auxiliary problem obtained at ϵ^a from the concentration equation.

$$\underbrace{\frac{1}{|Y|}\int_{Y_f}\nabla_t(C_{s0}+S_{d0})dy}_{I_1}-\underbrace{\frac{1}{|Y|}\int_{Y_f}\nabla_x.(D(t,y)(\nabla_x C_{s0}+\nabla_y C_{s1}))dy}_{I_2}-$$
$$\underbrace{\frac{1}{|Y|}\int_{Y_f}\nabla_y.(D(t,y)(\nabla_x C_{s1}+\nabla_y C_{s2}))dy}_{I_3}+\underbrace{\frac{1}{|Y|}\int_{Y_f}\nabla_x.(u_0C_{s0})dy}_{I_4}+$$
$$\underbrace{\frac{1}{|Y|}\int_{Y_f}\nabla_y.(u_0C_{s1})dy}_{I_5}=0 \tag{3.20}$$

By analysing I_1, I_2, I_3, I_4, I_5 using Gauss's theorem, the results in P_0^c and periodicity of the measured quantities we have

$$I_1 = \frac{|Y_f|}{|Y|}\nabla_t(C_{s0}+S_{d0}) \tag{3.21}$$
$$I_2 = \frac{1}{|Y|}\sum_{i=1}^{2}\nabla_{x_i}(\sum_{j=1}^{2}(\int_{Y_f}D(t,y)(\delta_{ij}+\nabla_{y_i}\chi_j^c(y))dy)\nabla_{x_j}C_{s0}) \tag{3.22}$$
$$I_3 = 0 \tag{3.23}$$
$$I_4 = \frac{|Y_f|}{|Y|}\nabla_x.(u_0C_{s0}) \tag{3.24}$$
$$I_5 = 0 \tag{3.25}$$

Denoting the porosity of the medium by $\phi=\frac{|Y_f|}{|Y|}$ we obtain from (3.20) the homogenized macroscopic model for concentration of soil particles with deposition as

$$\phi\frac{\partial}{\partial t}(C_{s0}+S_{d0})+\phi\nabla_x.(u_0C_{s0})=\nabla_x.(D^h\nabla_xC_{s0})\ in\ \Lambda \tag{3.26}$$

with the effective macroscopic diffusion coefficient

$$D^h=\frac{1}{|Y|}\sum_{j=1}^{2}(\int_{Y_f}D(t,y)(\delta_{ij}+\nabla_{y_i}\chi_j^c(y))dy),\ \ i=1,2 \tag{3.27}$$

3.3 Homogenization of the equation of motion of mixture

Next we homogenize the momentum equation by substituting (3.1) and (3.4) into (2.3) and (2.4) and collecting terms involving powers of ϵ.

3.3.1 Boundary value problem for u_0:

The lowest order of ϵ gives the auxiliary equation:

$$P_{-2}^u\begin{cases}Find\ u_0=u_0(t,x,y)\ such\ that\\ \nabla_y.2\mu(t,y)\nabla_y u_0=0\ in\ Y^f\\ 2\mu(t,y)\nabla_y u_0.n=0\ on\ \partial Y^s\\ u_0=u_0(t,x,y)\ is\ Y-periodic\end{cases} \tag{3.28}$$

P_a^u for $a\in\mathbf{R}$ similarly denote auxiliary problem obtained at ϵ^a from the momentum equation.

The solution to P^u_{-2} is of the form

$$u_0(t,x,y) = u_0(t,x) \tag{3.29}$$

3.3.2 Boundary value problem for u_1:

Simplifying the asymptotic expansion for the second order term u_1 we obtain the auxiliary problem P^u_{-1}

$$P^u_{-1}\begin{cases} Find\ u_1 = u_1(t,x,y)\ such\ that \\ -\nabla_y.(2\mu(t,y)(\nabla_x u_0 + \nabla_y u_1)) = 0\ in\ Y^f \\ 2\mu(t,y)(\nabla_x u_0 + \nabla_y u_1).n(y) = 0\ on\ \partial Y^s \\ u_1 = u_1(t,x,y)\ is\ Y-periodic \end{cases} \tag{3.30}$$

Equation (3.30) is linear and by separation of variables u_1 is a linear function of $\nabla_x u_0$, therefore we seek a solution of the form

$$u_1(t,x,y) = \bar{u}_1(t,x) + \sum_{k=1}^{2} \nabla_{x_k} u_0(t,x)\chi^u_k(y) \tag{3.31}$$

for cell function $\chi^u_k(y) \in \mathbf{R}^2$ which are solutions to the cell problem obtained by substituting (3.31) into (3.30)

$$P^u_{-1,k}\begin{cases} -\nabla_y.(2\mu(t,y)(\bar{e}_k + \nabla_y\chi^u_k(y)) = 0\ in\ Y^f \\ 2\mu(t,y)(\bar{e}_k + \nabla_y\chi^u_k(y)).n(y) = 0\ on\ \partial Y^s \\ \chi^u_k\ is\ Y-periodic \end{cases} \tag{3.32}$$

the cell function χ^u_k is a unique solution to $P^u_{-1,k}$ via Lax-Milgram theorem.

3.3.3 Boundary value problem for u_2:

After simplification using the results obtained in the system of equations ((3.11)-(3.13)) we get

$$P^u_0\begin{cases} \nabla_t u_0 - (u_0.\nabla_x)u_0 + E_u(t,y)\nabla_x p_o - \nabla_x.(2\mu(t,y)(\nabla_x u_0 + \nabla_y u_1)) - \\ \nabla_y.(2\mu(t,y)(\nabla_x u_1 + \nabla_y u_2)) = 0\ in\ Y^f \\ 2\mu(t,y)(\nabla_x u_1 + \nabla_y u_2).n(y) = 0\ on\ \partial Y^s \\ u_2(t,x,y)\ is\ Y-periodic \end{cases} \tag{3.33}$$

We proceed by integrating (3.33) over the unit cell Y and average with respect to y

$$\underbrace{\frac{1}{|Y|}\int_{Y_f}\frac{\partial u_0}{\partial t}dy}_{I_6} + \underbrace{\frac{1}{|Y|}\int_{Y_f}(u_0.\nabla_x)u_0 dy}_{I_7} + \underbrace{\frac{1}{|Y|}\int_{Y_f}E_u(t,y)\nabla_x p_0 dy}_{I_8} - \underbrace{\frac{1}{|Y|}\int_{Y_f}\nabla_x.(2\mu(t,y)(\nabla_x u_0 + \nabla_y u_1))dy}_{I_9} - \underbrace{\frac{1}{|Y|}\int_{Y_f}\nabla_y.(2\mu(t,y)(\nabla_x u_1 + \nabla_y u_2))dy}_{I_{10}} = 0 \tag{3.34}$$

Simplify (3.34) using the boundary condition in (3.33), Gauss's theorem and periodicity:

$$I_6 = \phi\frac{\partial u_0}{\partial t} \tag{3.35}$$

$$I_7 = \phi(u_0.\nabla_x)u_0 \tag{3.36}$$

$$I_8 = \bar{E}_u \nabla_x p_0 \ \ with \ \ \bar{E}_u = \frac{1}{|Y|}\int_{Y_f} E_u(t,y)dy \tag{3.37}$$

$$I_9 = \frac{1}{|Y|}\sum_{l=1}^{2}\nabla_{x_l}(\sum_{k=1}^{2}(\int_{Y_f} 2\mu(t,y)(\delta_{lk} + \nabla_{y_l}\chi_k^u(y))dy)\nabla_{x_k}u_0) \tag{3.38}$$

$$I_{10} = 0 \tag{3.39}$$

Consequently we obtain the homogenized macroscopic equation for the momentum equation under Lamina flow conditions as

$$\phi\frac{\partial u_0}{\partial t} + \phi(u_0.\nabla_x)u_0 + \bar{E}_u\nabla_x p_0 - 2\nabla_x.(\mu^h\nabla_x) = 0 \ \ in \ \ \Lambda \tag{3.40}$$

with the effective macroscopic molecular viscosity given by

$$\mu^h = \frac{1}{|Y|}\sum_{k=1}^{2}(\int_{Y_f}\mu(t,y)(\delta_{lk} + \nabla_{y_l}\chi_k^u(y))dy, \quad l = 1,2 \tag{3.41}$$

The concluding equations for rate of deposition and rate of decrease in fraction of non-clogging conduit respectively becomes

$$\frac{\partial S_{d0}}{\partial t} = (\beta_{nc}f_{nc_0} + \beta_{cl}(1 - f_{nc_0}))\Psi C_{s0} \ \ in \ \ \Lambda \tag{3.42}$$

$$\frac{\partial f_{nc_0}}{\partial t} + \beta_{nc}\Psi f_{nc_0}C_{s0} = 0 \ \ in \ \ \Lambda \tag{3.43}$$

It must be noted that through homogenization the microscale variable y has been averaged out of the homogenized equations which are now void of oscillations(ϵ) and are functions of the macroscale variable x and time t only. The highly oscillatory coefficients have been replaced with effective coefficients.

4 Numerical Computation of the Homogenized Model

We now apply the model to simulate the piping flow erosion with deposition within a highly erodible soil under a tangential flow instigated by seepage of water through the embankment. A constant pressure drop between inlet and outlet with a constant flux at the inlet was imposed, tangential velocities are supposed continuous across $\partial\Lambda$.

The finite element method (FEM) was used to discretize the cell problems and macroscopic equations, the algorithms are presented to clearly outline the computational processes involved. Meanwhile for a detailed report on FEM we refer the reader to [28]. A splitting method namely Incremental Pressure Correction Scheme (IPCS) was used to decouple the momentum equation as it is known to reduce computational cost with an improved time accuracy as compared to fully coupled schemes [29, 30, 31].

Table 2. Numerical values of parameters

L	H	p_{in}	ρ^w	ρ^p	ϕ
2m	1m	0.1	$1000kgm^{-3}$	$2700kgm^{-3}$	0.35
k_{er}	Ψ	β_{nc}	β_{cl}	E_u	C_{soil}
$0.01\ sm^{-1}$	$1.22\times10^{-6}ms^{-1}$	0.73	3.96×10^{-4}	0.00424	0.65

4.1 Initial and boundary conditions

We simulated the homogenized equations under the following conditions:

$$\begin{aligned} f_{nc_0}(0,x_1,x_2)=1, \quad S_{d0}(0,x_1,x_2)=0 \\ C_{s0}(t,0,x_2)=0, \quad S_{d0}(t,0,x_2)=0 \\ p_0(t,0,x_2)=p_{in}, \quad p_0(t,L,x_2)=0 \\ u_0(t,x_1,0)=0, \quad u_0(t,x_1,L)=0 \end{aligned}$$

Numerical values of the parameters used are given in Table 2 for a rectangular soil domain of dimensions $2m\times1m$ with highly erodible soil, whilst the characteristic erosion time was computed as in [23]. Thus $t_{er}=\dfrac{2L\rho^p}{k_{er}p_{in}}$ with a value of $3000hrs$.The mixture density $\rho=\phi(\rho^p-\rho^w)+\rho^w$, where ρ^w and ρ^p are water and soil particles density, compacity of the soil denoted $C_{soil}=1-\phi$.

4.2 Numerical procedure

The numerical method for the results on the homogenized equations are based on piecewise quadratic mixed Galerkin finite element algorithm on an unstructured triangular mesh. The time-stepping was performed using Backward Euler Method with a time step $\delta t=0.2$ for $0\le t\le 20$. The steps for numerically computing the homogenization procedure are as follows:

(i) Compute the cell problem:

$$-\frac{\partial}{\partial y_i}\left(D_{ik}(t,y)\frac{\partial\chi_j^c}{\partial y_k}\right)=\frac{\partial}{\partial y_i}D_{ij}(t,y)$$

$$B.C: \quad \left(D_{ij}(t,y)+D_{ik}(t,y)\frac{\partial\chi_j^c}{\partial y_k}\right).n(y)=0 \tag{4.1}$$

$$-\frac{\partial}{\partial y_i}\left(\mu_{ik}(t,y)\frac{\partial\chi_j^\mu}{\partial y_k}\right)=\frac{\partial}{\partial y_i}\mu_{ij}(t,y)$$

$$B.C: \quad \left(\mu_{ij}(t,y)+\mu_{ik}(t,y)\frac{\partial\chi_j^c}{\partial y_k}\right).n(y)=0 \tag{4.2}$$

for $i,k=1,2$,$j=1,2$ and $\chi_j^c,\chi_j^\mu-Y$ periodic

(ii) Compute the Homogenized effective characteristic coefficients:

$$D_{=}^h\frac{1}{|Y|}\int_{Y_f}\left(D_{ij}(t,y)+D_{ik}(t,y)\frac{\partial\chi_j^c}{\partial y_k}\right)dy \tag{4.3}$$

$$\mu_{=}^h\frac{1}{|Y|}\int_{Y_f}\left(\mu_{ij}(t,y)+\mu_{ik}(t,y)\frac{\partial\chi_j^u}{\partial y_k}\right)dy \tag{4.4}$$

$$\bar{E_u}=\frac{1}{|Y|}\int_{Y_f}E_u dy \tag{4.5}$$

for $i,k=1,2$,$j=1,2$

(iii) Solve the Homogenized problem 2D:

$$\phi\frac{\partial u_{0_i}}{\partial t}+\phi u_{0_j}\frac{\partial u_{0_i}}{\partial x_j}=-\bar{E}_u\frac{\partial p_0}{\partial x_i}+2\mu^h\frac{\partial^2 u_{0_i}}{\partial x_i^2} \tag{4.6}$$

$$\phi\frac{\partial C_{s0}}{\partial t}+\phi\frac{\partial S_{d0}}{\partial t}+\phi u_{0_j}\frac{\partial C_{s0}}{\partial x_j}=D^h\frac{\partial^2 C_{s0}}{\partial x_i^2} \tag{4.7}$$

for $i=1,2$,$j=1,2$

With concluding equations for deposition and pore space dynamics

$$\frac{\partial S_{d0}}{\partial t}=[\beta_{nc}f_{nc_0}+\beta_{cl}(1-f_{nc_0})]\Psi C_{s0} \tag{4.8}$$

$$\frac{\partial f_{nc_0}}{\partial t}+\beta_{nc}\Psi f_{nc_0}C_{s0}=0 \tag{4.9}$$

4.2.1 Finite element implementation of the cell problem

To compute χ^c in (4.1) a test space $\hat{Q}(Y)=\{\eta\in H^1(Y):\eta=0\ \ on\ \ \partial Y,\eta\ \ is\ \ Y-periodic\}$ and a trial space $Q(Y)=\{\chi_j^c\in H^1(Y):\chi_j^c=0\ \ on\ \ \partial Y,\chi_j^c\ \ is\ \ Y-periodic\}$ were chosen. Using the test function $\eta\in\hat{Q}(Y)$ and Greens theorem the weak formulation of (4.1) is

$$\begin{aligned}\int_Y-\frac{\partial}{\partial y_i}\left(D_{ik}(y)\frac{\partial}{\partial y_k}(\chi_j^c+y_j)\right)\eta dy \quad &= \\ \int_Y D_{ik}(y)\frac{\partial}{\partial y_k}(\chi_j^c+y_j)\frac{\partial\eta}{\partial y_i}dy-\int_{\partial Y}D_{ik}(y)\frac{\partial}{\partial y_k}(\chi_j^c+y_j)\eta.n_i dS &\end{aligned} \tag{4.10}$$

Since the test function is zero on the boundary, equation (4.10) simplifies to,

$$\int_Y D_{ik}(y)\frac{\partial}{\partial y_k}(\chi_j^c+y_j)\frac{\partial\eta}{\partial y_i}dy=0$$

Hence the bilinear form: Find $\chi_j^c\in Q(Y)$ such that

$$a_Y((\chi_j^c+y_j),\eta)=0 \tag{4.11}$$

for all $\eta\in\hat{Q}(Y)$. Next the unit cell Y was divided into P triangles T_p with G nodes P_i. Choose $\hat{Q}_h(Y)$ a finite dimensional subspace of $\hat{Q}(Y)$ of dimension g and a basis function $\eta_k\in\hat{Q}_h(Y)$, $k=1,2,...,g$. Using piecewise linear basis function, let $\eta_k(P_i)=\delta_{kl}$ and the approximate solution to (4.11) $\chi_j^c(y)_h=\sum_{k=1}^g\gamma_k^j\eta_k(y)\ \ for\ \ all\ \ y\in Y$ with γ_k^j constants. Also for $\eta\in\hat{Q}_h(Y)$ let $\eta=\sum_{i=1}^g\nu_i\eta_i$, ν_i constants. Hence (4.11) becomes the finite dimensional problem find $\chi_{j_h}^c\in Q_h(Y)$ such that

$$a_Y(\chi_{j_h}^c,\eta)=M_Y(\eta) \tag{4.12}$$

from which we obtain the system of equations

$$\sum_{k=1}^g A_{ik}\gamma_k^j=b_i^j,\ \ i=1,2,...,g,\ \ j=1,2 \tag{4.13}$$

where

$$A_{ik}=a_Y(\eta_k,\eta_i)=\int_Y D_{ij}(y)\frac{\partial\eta_k}{\partial y_j}\frac{\partial\eta_i}{\partial y_i}dy$$

and

$$b_i^j=M_Y(\eta_i)=\int_Y D_{ij}(y)\frac{\partial\eta_i}{\partial y_i}dy$$

Similarly for (4.2) we have the finite dimensional problem:
find $\chi^{\mu}_{j\,h} \in Q_h(Y)$ such that

$$b_Y(\chi^{\mu}_{j\,h}, \eta) = N_Y(\eta) \tag{4.14}$$

which gives the system of equations

$$\sum_{k=1}^{g} B_{ik}\alpha^j_k = d^j_i, \;\; i = 1, 2, ..., g, \;\; j = 1, 2, \;\; \alpha^j_k \;\; constants. \tag{4.15}$$

where

$$B_{ik} = b_Y(\eta_k, \eta_i) = \int_Y \mu_{ij}(y)\frac{\partial \eta_k}{\partial y_j}\frac{\partial \eta_i}{\partial y_i}dy$$

and

$$d^j_i = N_Y(\eta_i) = \int_Y \mu_{ij}(y)\frac{\partial \eta_i}{\partial y_i}dy$$

By defining $D_{ij}(t, y) = D_{ij}\delta_{ij}$, $\mu_{ij}(t, y) = \mu_{ij}\delta_{ij}$ and using the results from (4.12) and (4.14), we compute the homogenized effective diffusive coefficient and molecular viscosity

$$D^h = \frac{1}{|Y|}\int_{Y_f}\left(D_{ij} + D_{ik}\frac{\partial \chi^c_j(y)_h}{\partial y_k}\right)dy \tag{4.16}$$

$$\mu^h = \frac{1}{|Y|}\int_{Y_f}\left(\mu_{ij} + \mu_{ik}\frac{\partial \chi^u_j(y)_h}{\partial y_k}\right)dy \tag{4.17}$$

4.2.2 Finite element implementation of the momentum equation for the water/soil mixture

Defining a test space $\hat{Q}(\Lambda) = \{\xi_1 \in H^1(\Lambda) : \xi_1 = 0 \;\; on \;\; \partial\Lambda\}$ and a trial space $Q(\Lambda) = \{u_0 \in H^1(\Lambda) : u_0 = 0 \;\; on \;\; \partial\Lambda\}$. Equation (4.6) was decoupled into

$$\int_\Lambda \frac{\phi(u^\star_{0_i} - u^n_{0_i})}{\delta t}\xi_1 dx + \int_\Lambda \phi u^n_{0_j}\frac{\partial u^n_{0_i}}{\partial x_j}\xi_1 dx + \int_\Lambda T(u^{n+\frac{1}{2}}_{0_i}, p^n_0)\frac{\partial \xi_1}{\partial x_{0_i}}dx - \int_{\partial\Lambda} T(u^{n+\frac{1}{2}}_{0_i}, p^n_0)\xi_1.\mathbf{n}dx = 0 \tag{4.18}$$

$$\bar{E}_u\int_\Lambda \frac{\partial p^{n+1}_0}{\partial x_i}\frac{\partial q}{\partial x_i}dx = \bar{E}_u\int_\Lambda \frac{\partial p^n_0}{\partial x_i}\frac{\partial q}{\partial x_i}dx - \phi(\delta t)^{-1}\int_\Lambda \frac{\partial u^\star_{0_i}}{\partial x_i}qdx \tag{4.19}$$

$$\phi\int_\Lambda u^{n+1}_{0_i}\xi_1 dx \;\; = \;\; \int_\Lambda u^\star_{0_i}\xi_1 dx - \delta t\bar{E}_u\int_\Lambda\left(\frac{\partial p^{n+1}_0}{\partial x_i} - \frac{\partial p^n_0}{\partial x_i}\right)\xi_1 dx \tag{4.20}$$

for test function q and a tentative velocity $u^\star$.

Choosing $\hat{Q}_h(\Lambda)$ a finite dimensional subspace of $\hat{Q}(\Lambda)$ of dimension g and piecewise quadratic basis functions $q_k, \xi_{1_k} \in \hat{Q}_h(\Lambda)$, $k = 1, 2, ..., g$, we let $q_k(P_i) = \delta_{kl}$, $\xi_{1_k}(P_i) = \delta_{kl}$ and the approximate solutions $p_{0_h}(t, x) = \sum_{k=1}^g \lambda^j_{1_k} q_k(x) \;\; for \;\; all \;\; x \in \Lambda$ and $u_{0i_h}(t, x) = \sum_{k=1}^g \lambda^j_{2_k}\xi_{1_k}(x) \;\; for \;\; all \;\; x \in \Lambda$ with $\lambda^j_{1_k}, \lambda^j_{2_k}$ constants. Also for $q_k, \xi_{1_k} \in \hat{Q}_h(\Lambda)$ let $\xi_1 = \sum_{i=1}^g \nu_{1_i}\xi_{1_i}$ and $q = \sum_{i=1}^g \nu_{2_i}q_i$, ν_{1_i}, ν_{2_i} constants.

We thus have from (4.18), (4.19), (4.20) the systems of equation

$$\int_\Lambda \frac{\phi(\xi^\star_{1_k} - \xi^n_{1_k})}{\delta t}\xi_{1_i}dx + \int_\Lambda \phi\xi^n_{1_k}\frac{\partial \xi^n_{1_k}}{\partial x_j}\xi_{1_i}dx + \int_\Lambda T(\xi^{n+\frac{1}{2}}_{1_k}, q^n_k)\frac{\partial \xi_{1_i}}{\partial x_i}dx - \int_{\partial\Lambda} T(\xi^{n+\frac{1}{2}}_{1_k}, q^n_k)\xi_{1_i}.\mathbf{n}dx = 0 \tag{4.21}$$

$$\bar{E}_u \int_\Lambda \frac{\partial q_k^{n+1}}{\partial x_i}\frac{\partial q_i}{\partial x_i}dx = \bar{E}_u \int_\Lambda \frac{\partial q_k^{n}}{\partial x_i}\frac{\partial q_i}{\partial x_i}dx - \phi(\delta t)^{-1}\int_\Lambda \frac{\partial \xi_{1_k}^{\star}}{\partial x_i}q_i dx \tag{4.22}$$

$$\phi\int_\Lambda \xi_{1_k}^{n+1}\xi_{1_i}dx \quad = \quad \int_\Lambda \xi_{1_k}^{\star}\xi_{1_i}dx - \delta t\bar{E}_u\int_\Lambda\left(\frac{\partial q_k^{n+1}}{\partial x_i} - \frac{\partial q_k^{n}}{\partial x_i}\right)\xi_{1_i}dx \tag{4.23}$$

4.2.3 Finite element implementation of the equation for soil particle concentration with deposition in the water/soil mixture

Similarly lets define test and trial space respectively as $\hat{V}(\Lambda) = \{\xi_2, \xi_3, \xi_4 \in H^1(\Lambda) : \xi_2 = \xi_3 = \xi_4 = 0 \ on \ \partial\Lambda\}$ and $V(\Lambda) = \{C_{s0}, S_{d0}, f_{nc_0} \in H^1(\Lambda) : C_{s0} = S_{d0} = f_{nc_0} = 0 \ on \ \partial\Lambda\}$ for $\hat{V}_h(\Lambda)$ a finite dimensional subspace of $\hat{V}(\Lambda)$ of dimension g and basis functions $\xi_{2_k}, \xi_{3_k}, \xi_{4_k} \in \hat{V}_h(\Lambda)$, $k = 1, 2, ..., g$. Using piecewise linear basis function we let $\xi_{2_k}(P_i) = \delta_{kl}$, $\xi_{3_k}(P_i) = \delta_{kl}$, *and* $\xi_{4_k}(P_i) = \delta_{kl}$ and the approximate solutions

$$C_{s0_h}(t,x) = \sum_{k=1}^{g}\lambda_{3_k}^{j}(x)\xi_{2_k} \quad for \ \ all \ \ x \in \Lambda$$

$$S_{d0_h}(t,x) = \sum_{k=1}^{g}\lambda_{4_k}^{j}(x)\xi_{3_k} \quad for \ \ all \ \ x \in \Lambda$$

$$f_{nc_{0h}}(t,x) = \sum_{k=1}^{g}\lambda_{5_k}^{j}(x)\xi_{4_k} \quad for \ \ all \ \ x \in \Lambda$$

with $\lambda_{3_k}^{j}, \lambda_{4_k}^{j}, \lambda_{5_k}^{j}$ constants Also for $\xi_{2_k}, \xi_{3_k}, \xi_{4_k} \in \hat{V}_h(\Lambda)$ we let $\xi_2 = \sum_{i=1}^{g}\nu_{3_i}\xi_{2_i}$
$\xi_3 = \sum_{i=1}^{g}\nu_{4_i}\xi_{3_i}, \xi_4 = \sum_{i=1}^{g}\nu_{5_i}\xi_{4_i}$, for $\nu_{3_i}, \nu_{4_i}, \nu_{5_i}$ constants. The system of equations are thus

$$\phi\int_\Lambda \frac{\xi_{2_k}^{n+1} - \xi_{2_k}^{n}}{\delta t}\xi_{2_i}dx + \phi\int_\Lambda \frac{\xi_{3_k}^{n+1} - \xi_{3_k}^{n}}{\delta t}\xi_{2_i}dx + \phi\int_\Lambda \xi_{1_k}^{n+1}\frac{\partial \xi_{2_k}^{n+1}}{\partial x_j}\xi_{2_i}dx$$
$$+D^h\int_\Lambda \frac{\partial \xi_{2_k}^{n+1}}{\partial x_i}\frac{\partial \xi_{2_i}}{\partial x_i}dx = 0 \tag{4.24}$$

$$\int_\Lambda \frac{\xi_{3_k}^{n+1} - \xi_{3_k}^{n}}{\delta t}\xi_{3_i}dx - \int_\Lambda [\beta_{nc}\xi_{4_k}^{n+1} + \beta_{cl}(1 - \xi_{4_k}^{n+1})]\Psi\xi_{2_k}^{n+1}\xi_{3_i}dx = 0 \tag{4.25}$$

$$\int_\Lambda \frac{\xi_{4_k}^{n+1} - \xi_{4_k}^{n}}{\delta t}\xi_{4_i}dx + \beta_{nc}\Psi\int_\Lambda \xi_{4_k}^{n+1}\xi_{2_k}^{n+1}\xi_{4_i}dx = 0 \tag{4.26}$$

4.3 Numerical results and discussion

The results in Fig. 2 was obtained on the unit cell under periodic boundary conditions.

Under the assumption that the geometry of the problem is symmetric, the effective molecular viscosity and diffusion coefficient are isotropic thus $D_{ij}(t,y) = D_{ij}\delta_{ij}$, *and* $\mu_{lk}(t,y) = \mu_{lk}\delta_{lk}$, $y \in Y$, we used the computed cell values to calculate the effective coefficients from (3.26) and (3.40) as

$$D^h = \begin{pmatrix} 0.0196 & 0 \\ 0 & 0.0196 \end{pmatrix} \quad \mu^h = \begin{pmatrix} 0.0031 & 0 \\ 0 & 0.0031 \end{pmatrix} \tag{4.27}$$

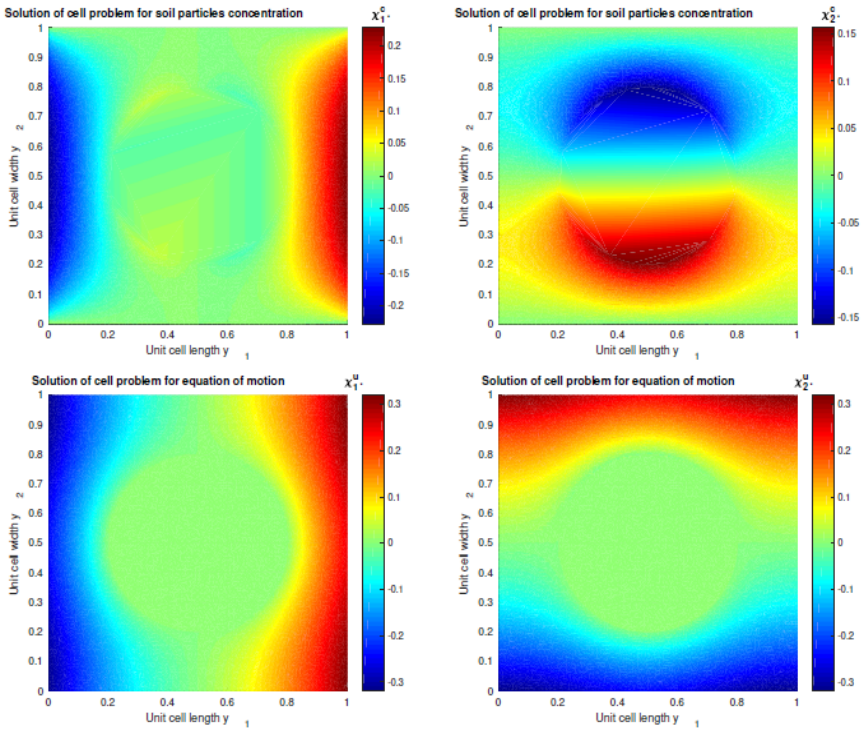

Fig. 2. Solution to cell problem for concentration of soil particles and momentum equation

The cell values in Fig. 2 are local variation in solute concentration and flow velocity created by the macroscopic gradient. The macroscopic homogenized equations are used to verify the development of the piping flow phenomena with deposition results of which are illustrated in Figs. 3-6.

For piping to occur there must be a seepage flow path and a source of water, erodable material within the flow path and an unprotected exit. We therefore describe an inflow at $x_1 = 0$ and an unprotected outflow at $x_1 = 2$ with the walls $x_2 = 0$ and $x_2 = 1$.The soil domain was subject to a constant pressure drop of 0.1 whose gradient is depicted in Fig. 3. The flow velocity profile was parabolic with the velocity increasing towards the middle portions. Higher shear values at the walls contributes to decreasing velocities and viscous regimes. As the pressure balances wall shear stress the velocity profile remain unchanged as shown in Fig. 3 from $\frac{t}{t_{er}} = 12$.

We studied the evolution of soil particle concentration for the chosen dimensionless time period. Our model clearly depicted the variations in soil particle concentration in mixture as expected from the heterogeneities of the medium as different levels of soil concentration were recorded through time and space. Accumulated eroded soil particles transformed the flow into a concentrated suspension with $\frac{C_{s0}}{C_{soil}}$ rising to a maximum of 1 from inflow to outflow for $0 < \frac{t}{t_{er}} \leq 4$ as shown in Fig. 4. These higher values of output soil concentration in flow lead to output hole enlargement. The simulations performed clearly show soil particle concentration in mixture decreasing with time,

experimental studies commonly project decreasing concentrations however we observed from our simulations that the particle concentration decreases at a decreasing rate becoming almost constant with time showing glimpses of dilute flow.

Significant deposition was recorded from the simulation though at lower levels as compared with the soil compacity. From Fig. 5 we observe a rapid increase in deposition for $0 < \frac{t}{t_{er}} \leq 12$, deposits further increased but at a slower rate. We noticed from the numerical studies that under Lamina flow conditions deposition increases over time but at a decreasing rate and there is a direct relationship between soil particles concentration in the mixture and soil particles deposition.

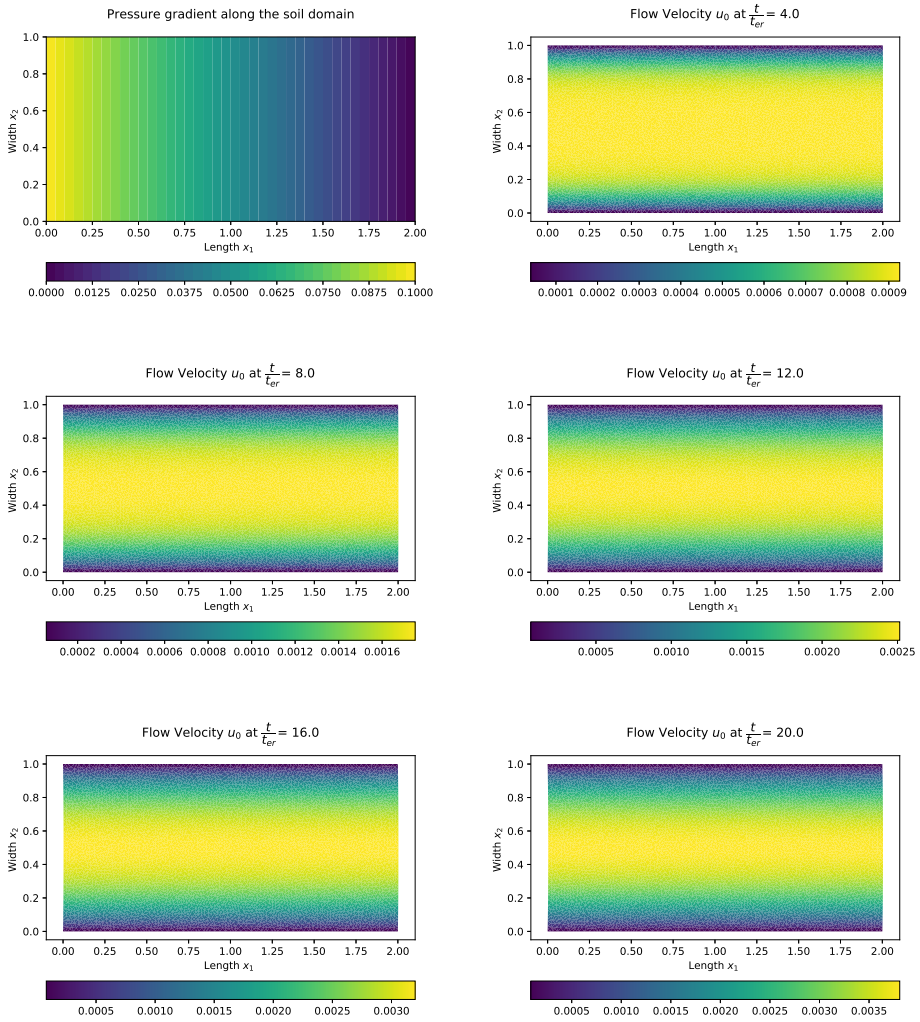

Fig. 3. Pressure and velocity profile in the soil domain

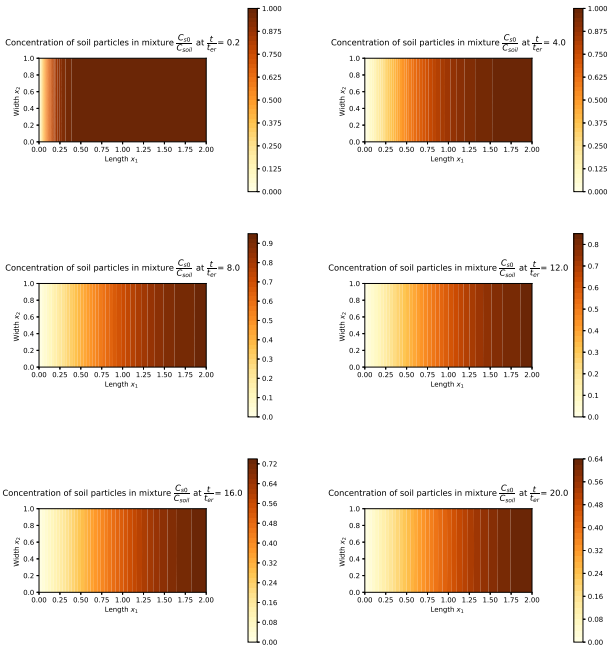

Fig. 4. Concentration of soil particles in water-soil mixture as a fraction of compacity of the soil domain

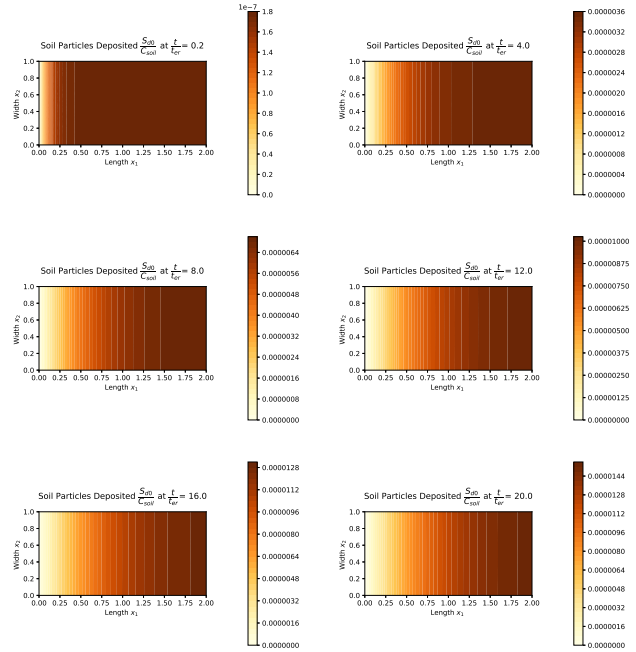

Fig. 5. Soil particles deposition in flow paths as a fraction of compacity of soil

With the assumption that prior to erosion the fraction of bare pore spaces is 1. We observed from the numerical studies a gradual decrease in this fraction with comparatively higher decreasing fractions at downstream part of the soil domain as in Fig. 6. The overall bare pore spaces in the entire soil domain was altered by the erosion which can be attributed to the deposits. Hence if filters are to be employed in embarkment treatment we recommend priority be given to regions closer to the inflow.

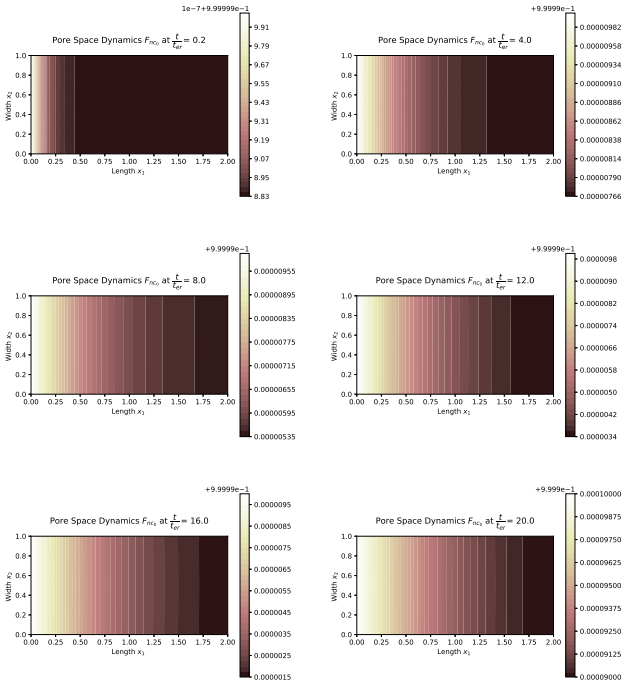

Fig. 6. Reduction in bare pore spaces as entrainment and deposits occur

5 Conclusion

In this study we investigated the effect of soil concentration in an erodable soil domain and how spatial variabilities and oscillating viscosity and diffusion could be homogenized using the homogenization process. We have presented a model which eliminates the assumptions of homogeneity and no deposition placed on the numerical modeling of the piping flow phenomena and hence our formulation provides a better representation of piping flow erosion. A system of classifying regions of clogged and nonclogging conduits in the soil domain was introduced. Numerical simulations for piping flow erosion with deposition in a spatially heterogeneous soil were conducted and the numerical results clearly show the various trends associated with soil particle concentration in the piping phenomena.

Competing Interests

Authors have declared that no competing interests exist.

References

[1] Bajin Pobia. Sixty-five percent of Ghana's land area is prone to soil erosion and desertification. Retrieved from Ghana News Agency; 2017.
Available:https://desertification.wordpress.com/2017/03/20

[2] Thomas Naadi. Ghana's coastal erosion: The village buried in sand; 2016.
Available:http://www.bbc.com/news/world-africa-36257360

[3] Kwasi Appeaning Addo. Coastal erosion in Ghana: Causes and effects. Nova Science Publishers. 2015;83-106.

[4] Kenneth Ruddle. The potential role of integrated management of natural resources in improving the nutritional and economic status of resource - poor farm households in Ghana. Research for the Future Development of Aquaculture in Ghana. 1996;42:94.

[5] Borrelli P, Robinson DA, Fleischer LR. An assessment of the global impact of 21st century land use change on soil erosion. Nature of Communications. 2017;8.

[6] ILIT. Investigation of the performance of the new orleans flood protection systems in hurricane katrina. Independent Levee Investigation Team, Report No. UCB/CCRM-06/01; 2006.

[7] Asumadu-Sarkodie Samuel, Owusu Phebe, Rufanga Patrick. Impact analysis of flood in Accra, Ghana . Advances in Applied Science Research. 2015;6:53-78.

[8] Stephane Bonelli, Olivier Brivois, Roland Borghi, Nadia Benahmed. Homogenization and two-scale convergence. C. R. Mecanique. 2006;334:555-559.

[9] Wilson GV Neiber JL, Sidle RC, Fox GA. Internal erosion during soil pipeflow: State of the science for experimental and numerical analysis. American Society of Agricultural and Biological Engineers. 2012;56:465-478.

[10] Velleux M, England J, Julien P. Spatially distributed model to assess watershed contaminant transport and fate. Science of the Total Environment. 2008;404(1):113-128.

[11] Sharif AR, Atkinson JF. Model for surface erosion of cohesive soils. Journal of Hydraulic Engineering. 2012;138(7):581-590.

[12] Mohammad H, Assefa MM, Hector RF. Erosion and sediment transport modelling in shallow waters: A Review on approaches, models and applications. Int J Environ Res Public Health. 2018;15(3):518.

[13] Wan CF, Fell R. Investigation of rate of erosion of soils in embankment dams. Journal of Geotechnical and Geoenvironmental Engineering. 2004;30:373-380.

[14] Fell R, Wan R, Cyganiewicz C, Foster M. Time for development of internal erosion and piping in embankment dams. Journal of Geotechnical and Geoennvironmental Engineering. 2003;334:129-307.

[15] Foster M, Fell R. MS. The statistics of embankment dam failures and accidents. Canadian Geotechnical Journal. 2000;37:1000-1024.

[16] Jones JAA, Richardson JM, Jacob JH. Factors controlling the distribution of piping in Britain : A reconnaissance survey. Geomorphology. 1997;20:289-306.

[17] Baihua Fu, Newham TH, Ramos-Scharron CE.. A review of surface erosion and sediment delivery models for unsealed roads. Environmental Modeling and Software. 2010;25:1-14.

[18] Yue Liang, Jun-jie Wang, Ming-wei Liu. Two-flow model for piping erosion based on liquid-solid coupling. J. Cent. South Univ. 2013;20:2299-2306.

[19] Soonkie Nam, John Petrie, Panayiotis Diplas. Effects of spacial variability on the estimation of erosion rrate fro cohesive riverbanks. Bundesanstalt fur Wasserbau. 2010;20.

[20] Scott Anderson, Keith Fergusion. Examination of three-dimensional effects of internal erosion and piping processes in soil; 2015.

[21] Vardoulakis I, Papanastasiou P, Stavropoulou M. Sand erosion in axial flow conditions. Transport Porous Medium. 2001;45:267-281.

[22] Van Beek VM, Hoffmans GJCM. Evaluation of dutch backward erosion piping models and a future perspective. 25th Meeting of the European Working Group on Internal Erosion; 2017.

[23] Lachouette D, Golay F, Bonelli S. One dimensional modelling of piping flow erosion. Mecanique CR. 2008;336:731-736.

[24] Bakhvalov N, Panasenko G. Homogenization: Averaging processes in periodic media. Kluwer, Dordrecht; 1989.

[25] Babuska I. Solution of interface problems by homogenization, I, II, III. SIAM J. Math.Anal. 1976;7:603-645.

[26] Nguetseng G. A general convergence result for a functional related to the theory of homogenization. SIAM J. Math. Anal. 1989;20:608-623.

[27] Gregoire Allaire. Homogenization and two-scale convergence. SIAM. J. Math. Anal. 1992;23:1482-1518.

[28] Mark S. Gockenbach. Understanding and implementing the finite element method. SIAM. 2006;57-63.

[29] Lorenzo Botti, Daniele A, Di Pietro. A pressure-correction scheme for convection-dominatedincompressible flows with discontinuous velocity and continuous pressure. Journal of Computational Physics; 2010.

[30] Chorin AJ. Numerical solution of the Navier-Stokes equations. Math. Comp. 1968;22:745-762.

[31] Saleri F, Veneziani A. Pressure-correction algebraic splitting methods for the incompresible Navier Stokes equations. SIAM Journal on Numerical Analysis. 2005;43:174-194.

Peer-review history:
The peer review history for this paper can be accessed here (Please copy paste the total link in your browser address bar)
http://www.sdiarticle4.com/review-history/56986